

Modal analysis of rotating carbon nanotube infused composite beams

C. DeValve¹, N. Ameri², P. Tarazaga³, R. Pitchumani^{1,*}

¹*Advanced Materials and Technologies Laboratory*

³*Center for Intelligent Material Systems and Structures*

Department of Mechanical Engineering

Virginia Tech

Blacksburg, VA, USA 24061-0238

²Department of Aerospace Engineering

University of Bristol

Senate House, Tyndall Avenue, Bristol BS8 1TH, UK

*Author for correspondence; Email: pitchu@vt.edu • Phone: 540 231 1776 • Fax: 540 231 9100

ABSTRACT

This study presents an operational modal analysis of rotating Carbon Nanotube (CNT) infused composite beams in order to explore the effect of CNT's on the natural frequencies and damping characteristics of the composite structure during rotation. Engineering applications with rotating components made from composites often suffer from excess vibrations because of the inherent high stiffness to weight ratio of the composite material and the oscillating loads from rotation. Previous research has demonstrated that the addition of CNT's to composite resins increases the damping characteristics of the resulting material, and several of these works have suggested that CNT-infused composites may be useful in rotor design as a means of passive vibration suppression. The present work aims to address this suggestion with an experimental investigation using composite beams fabricated with CNT's embedded in an epoxy resin matrix along with several layers of reinforcing carbon fiber fabric. An experimental apparatus is designed and constructed to hold two cantilever composite beams on opposite sides of a rotating central shaft controlled via a DC servo motor and a PID control loop. White noise is generated and added to the input motor RPM signal to randomly excite the base of the structure during rotation, and the Eigensystem Realization Algorithm (ERA) is used to analyze the data measured from the vibrating beam in order to determine the modal parameters of the system. The extracted modal parameters are presented as a function of the angular speed and weight percentage CNT loading in order to gain insight into application areas involving vibration suppression in rotating composite structures such as helicopter rotors and wind turbine blades.

Keywords: operational modal analysis, eigensystem realization algorithm, carbon nanotube damping, fiber-reinforced composite, rotating structure

INTRODUCTION

As the implementation of fiber-reinforced composite materials in engineering applications continues to increase, it is important to explore the potential benefits that can be designed into the physics of these materials. Much research has begun to explore the advantages of adding Carbon Nanotubes (CNT's) to the matrix of composite materials, such as strength and stiffness enhancement [1,2], increased fracture and impact resistance [3,4], thermal and electrical conductivity improvement [5], and material damping augmentation [6–8]. Damping improvement and the consequent reduction of vibrations is often critical to the successful operation of engineering structures which are composed of composite materials, for instance robotic

arms, automotive and aerospace panels, helicopter rotors, and wind turbine blades. Reducing vibrations in rotating composite structures such as the aforementioned helicopter rotors or wind turbine blades is essential to maximizing the performance and lifespan of these structures while minimizing their adverse effects on surrounding individuals. Currently, the majority of vibration suppression methods in rotating composite structures consist of complex active techniques that add weight and intricacy to the structure, and therefore a passive means of vibration suppression built into the composite material of these rotors would be beneficial.

Previous research has shown that there is a weak interfacial bond at the CNT-matrix interface when CNT's are incorporated into thermosetting composite matrices [9], which has been sought to be remedied by methods such as CNT surface functionalization [10], [11]. Although this weak interfacial bond may be seen as a material defect, this characteristic can alternatively be exploited since a stick-slip action resulting in energy dissipation can occur at the CNT-matrix interface as the material is put under strain [12], [13]. Experimental measurements have supported this theory by demonstrating that the damping in CNT-reinforced composites increases with increasing strain [6], [7], [14]. Considering that a rotating structure is subject to increased loads and strains due to rotation-induced forces, it is reasonable to infer that the CNT damping mechanism described above has the potential to provide a significant damping enhancement to rotating composite structures during operation when increased strains are present. Building upon this idea, the current work presents an experimental study which investigates the effects of matrix-embedded CNT's on the modal parameters of rotating fiber-reinforced composite systems, using Operational Modal Analysis (OMA) techniques [12,13] and the Eigensystem Realization Algorithm (ERA) [17] to analyze data measured from rotating cantilever composite beams.

METHOD

The experimental investigation focuses on rotating fiber-reinforced CNT-infused composites in order to explore the influence of CNT's on the modal properties of functional engineering composite structures. Single-Walled Carbon Nanotubes (SWCNT's) are used in the present study, which were purchased from SES Research (Houston, TX) with >90% purity and dimensions of <2 nm in diameter and 5–15 μm in length. The composite samples were made via hand layup and compression molding, and the cured three-part composites were tested using an in-house developed experimental test setup and a proprietary ERA code developed at the University of Bristol.

Composite Fabrication

The thermosetting-matrix fiber-reinforced SWCNT-infused composite samples were fabricated using compression molding techniques in which the resin flows through the thickness of the part as it is being compressed to ensure uniformity of CNT dispersion throughout the sample. The CNT-epoxy mixture was prepared as follows: First, EPON 826 resin (Hexion Specialty Chemicals, Columbus OH) was mixed with Heloxy Modifier 68 (Hexion Specialty Chemicals, Columbus OH) with a ratio of 4:1 by weight in order to reduce the viscosity of the EPON 826 resin. Appropriate amounts of this resin mixture and CNT's were then weighed into a beaker using an Ohaus Explorer Pro balance to achieve the appropriate weight percentage of the CNT's in the final epoxy. The nanotubes were then delicately mixed into the resin by hand using a medical grade utensil in order to ensure that the CNT's were integrated with the resin before transport from the balance. After this brief manual stirring, the resin-CNT combination was blended using a IKA T25 high-shear mixer for 90 seconds. A Cole-Parmer 500 watt ultrasonic processor with the appropriate size probe was then used to process the sample using a pulsed on-off mode with one second pulses for a total processing time of five minutes. The appropriate amount of hardener was then added to the sample and immediately incorporated with the CNT-resin sample using manual stirring for two minutes and the high-shear mixer for an additional 90 seconds. The entire resin sample was then transferred to a larger diameter beaker to increase the exposed surface area of the resin and degassed for 30 minutes.

The composite beams were fabricated using a hand-layup technique and compression molded using a 3-part aluminum mold consisting of a separable top section, a middle spacer frame, and a bottom plate, presented in the left and center portions of Figure 1, along with a finished composite plate shown on the far right-hand side of the figure. The top and bottom mold sections were sealed to the middle spacer using an O-ring fitted to a machined groove in each respective piece. A 3K plain weave carbon fiber fabric (Fibre Glast Development Corp, Brookville OH), with 12.5 picks and wefts per inch, a nominal thickness of 0.3 mm, and an areal weight of 193 g/m² was used as the reinforcement fabric. Precise amounts of the epoxy-

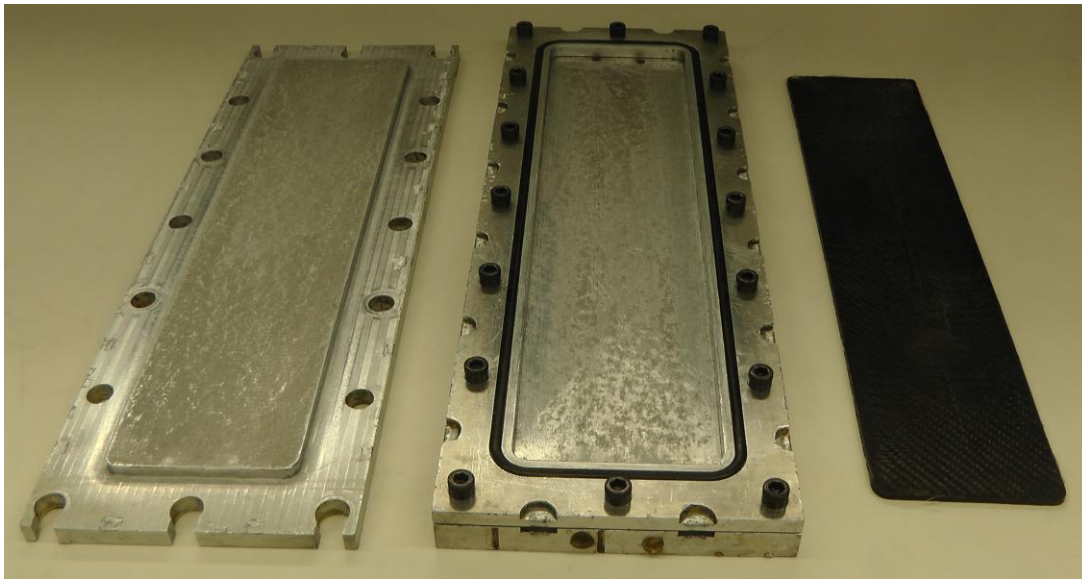


Figure 1: The three part aluminum mold used to fabricate the composite samples, where the top of the mold is shown on the left-hand side of the figure and the center spacer bolted to the bottom plate is shown in the figure's center. On the right-hand side of the figure a finished CNT-infused carbon fiber reinforced composite plate is shown after being cured and removed from the mold.

CNT mixture was poured between every two layers of carbon fiber fabric during the hand layup to minimize any filtering of the CNTs from the epoxy during the resin-permeation stage of the compression molding process. The sample was then processed using a programmable hot press from Tetrahedron Associates (San Diego, CA) using the following cure cycle: First, the mold was held at 40 °C and 40 kN for 1 hour. The mold was then held under the same force while the temperature was ramped to 120 °C over a ten minute period. After 2 hours at 40 kN and 120 °C, the mold was then cooled to room temperature in 15 minutes and the composite specimen was removed from the mold and machined into long slender beams of dimensions 266 x 12.7 x 0.2 mm to be used in the experimental rotating test stand.

Rotating Test Stand

An experimental test rig was developed to rotate two cantilever beams up to angular velocities of 500 RPM and simultaneously monitor the vibration of the beams during operation, depicted in Figure 2a. The test rig control interface developed using Labview™ 9.0 is presented in Figure 2b, which also graphically displays the angular speed of the motor and the accelerometer measurements in real time. To rotate the beams, a brushed DC motor (Magmotor, Worcester, MA) was mounted to the underside of a raised aluminum plate and controlled via a PID algorithm developed in Labview. Attached to the central rotating shaft of the motor was a fixture consisting of two clamps on opposite sides of the shaft in order to mount the cantilever beams, where the beams extended lengthwise parallel to the plane of rotation with their primary transverse vibrations also occurring parallel to the plane of rotation. Two accelerometers were attached to one of the beams, the first monitoring the acceleration at the tip of the beam (fixed) where the second (roving) was positioned variably along the length of the beam at precise increments during different experimental measurements. To minimize the effect of inter-sample variation from the roving accelerometer, washers of equal size and mass were attached to the beam at each unused accelerometer node location during the data acquisition. The accelerometers were powered by an external current source, and the signal from the test rig was passed through a liquid mercury slip ring at the top of the rotating test stand and fed through an analog Low-Pass (LP) filter before being recorded by Labview. Vibration measurements were recorded from the test setup at angular speed values from 0 to 500 RPM in 100 RPM increments, where 30 seconds of continuous data sampled at a rate of 1800 Hz with an equivalent LP filter value was recorded in each case. Uniform white noise of +/- 10 RPM was added to the constant angular speed signal sent to the motor in order to randomly excite the base of the beam during operation and approach excitation conditions that maximize the effectiveness of OMA analysis techniques. The acquired data was then compiled and analyzed using ERA, detailed in the next subsection.

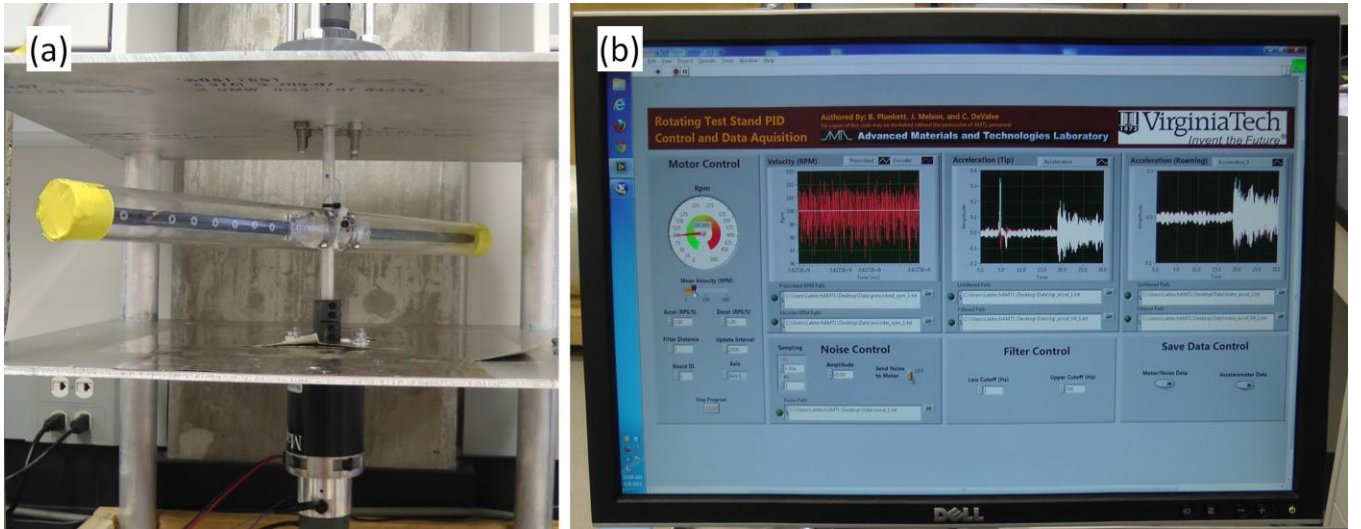


Figure 2: Depiction of the (a) rotating test rig and (b) Labview™ user control interface.

Eigensystem Realization Algorithm (ERA)

In this work, the Eigensystem Realization Algorithm (ERA) is used for the estimation of modal parameters from output-only measurements. ERA is a time-domain technique originally aimed at the evaluation of the dynamic behavior of structures from impulse responses. The discretized state space formulation [18] is defined as follows:

$$\begin{aligned} \mathbf{x}(k+1) &= \mathbf{A}\mathbf{x}(k) + \mathbf{b}(k) \\ \mathbf{y}(k) &= \mathbf{C}\mathbf{x}(k) \end{aligned} \quad (1)$$

where $\mathbf{x}(k)$ is the state vector at the time instant $t(k) = k\Delta t$, $\mathbf{y}(k)$ is the output vector, \mathbf{A} and \mathbf{C} are the state and output matrix respectively, and \mathbf{b} is the input to the system (assumed null after the initial time for an impulse response). The estimation of the modal parameters are evaluated by calculating the eigenvalues and the eigenvectors of the state space matrix \mathbf{A} . An essential step for the estimation of the state space matrix is the evaluation of the Hankel matrix which collects the impulse response of the system at shifted time steps, written as:

$$\mathbf{H}(k) = \begin{bmatrix} \mathbf{h}_k & \mathbf{h}_{k+1} & \cdots & \mathbf{h}_{k+q-1} \\ \mathbf{h}_{k+1} & \mathbf{h}_{k+2} & \cdots & \mathbf{h}_{k+q} \\ \vdots & \vdots & \ddots & \vdots \\ \mathbf{h}_{k+p-1} & \mathbf{h}_{k+p} & \cdots & \mathbf{h}_{k+q+p-2} \end{bmatrix} \quad (2)$$

where \mathbf{h}_k is a vector that contains the impulse responses at time instant k .

The relationship presented in [19] allowed the extension of this technique to the OMA case. Assuming that a system is excited by stationary white noise, it has been shown that the correlation function $R_{ij}(t)$ between the response signals i and j at a time interval of t is similar to the response of the structure at i due to an impulse at j . Assuming damping to be small, this is expressed by the relation

$$R_{ij}(k\Delta t) = \sum_{r=1}^{2N} C_{ij}^{(r)} e^{s_r k\Delta t} \quad (3)$$

where $C_{ij}^{(r)}$ is a constant associated with the r -th mode for the j -th response signal (i.e. the reference signal) and s_r is the system pole. This expression allows the use of techniques such as single-reference or poly-reference Least Square Complex Exponential (LSCE) methods, the Ibrahim time-domain method (ITD), and the eigensystem realization algorithm (ERA). Specifically for the ERA case, elements of the matrix in Eq. 2 can be substituted with correlation functions and applied to estimate the modal parameters of the system.

RESULTS AND DISCUSSION

As the goal of this work is to investigate the effect of matrix-embedded CNT's on the modal parameters of fiber-reinforced composites during rotation—with a particular focus on the damping enhancement as a result of the addition of CNT's to the epoxy matrix—the following results present the natural frequencies and damping values of the composite beams found from the ERA analysis as a function of the CNT weight percent loading and angular excitation speed. The following OMA analysis is still in a preliminary development stage and will be expounded in future research.

Experimental Test Setup Validation

Extensive work was conducted to validate the rotating experimental test rig by studying the effects of clamping on the modal parameter measurements of various beams. Aluminum was used as a baseline material based on the large quantity of available literature detailing its damping characteristics [20–22], and several beams were machined out of 2024 aluminum to match the dimensions of the composite beams described above. Modal hammer and base excitation tests were performed on the beams using free-free and clamped-free boundary conditions with several different clamps. The frequency response of the materials were recorded in each case and the damping in the first mode was calculated as a comparison metric, where the results are presented in Figures 3 and 4.

Figure 3 presents a frequency response plot for an aluminum beam (Fig. 3a) and a composite beam with no CNT's (Fig. 3b) obtained from an impact hammer test using an in-house fabricated stationary mounted clamp (denoted as clamp 1) compared to the clamp used on the rotating test stand. The frequency response measurements appear similar in each respective case shown in Fig. 3, with the first three natural frequencies occurring at approximately 20, 118, and 334 Hz in the aluminum beam and 21, 125, and 345 Hz in the composite beam with no CNT's. The difference in the first and second natural frequency measurements between the two different clamps equals about 1% for both beams, and a variation of about 5% is seen in the measured third natural frequencies for both beams between the two different clamps, which indicates good agreement between the two different clamping fixtures.

Additional tests were carried out using the same aluminum beam and composite beam with no CNT's to calculate the damping in the first mode of these respective materials and determine the influence from different testing methods and boundary conditions on the computed results, where the full validation test matrix is summarized in Table 1 and the results

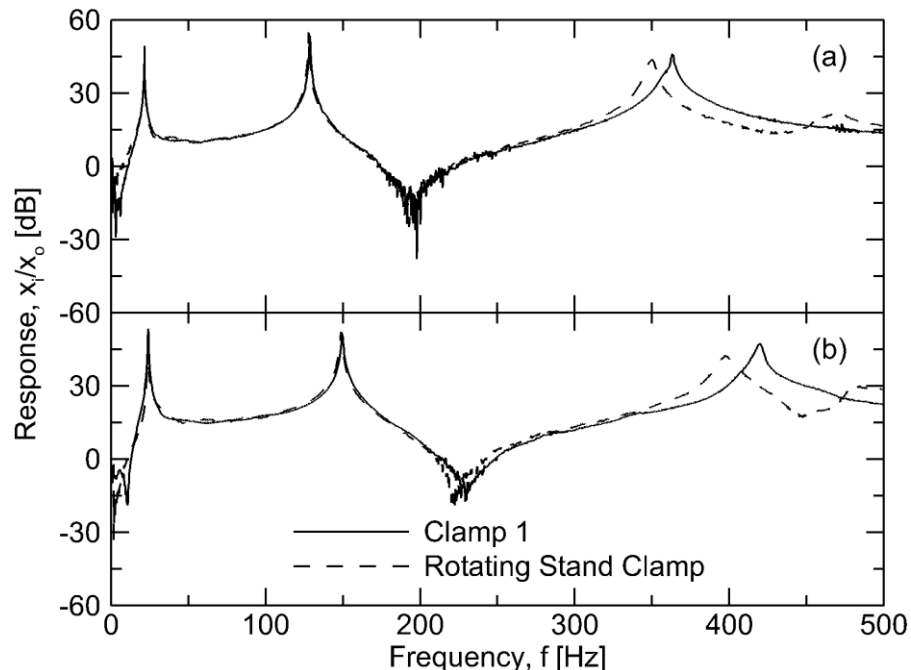
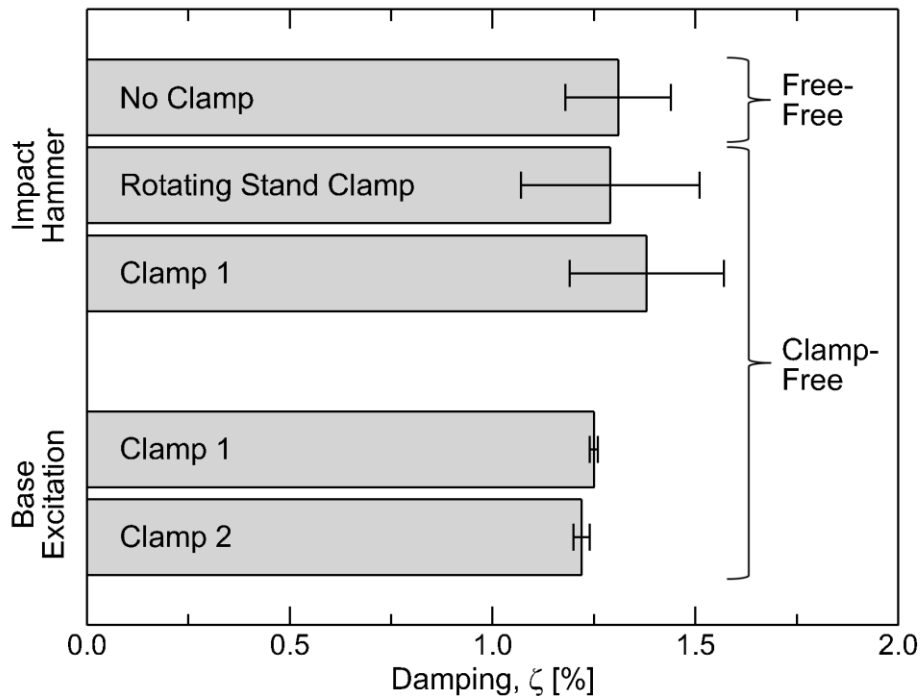


Figure 3: Frequency response of the clamped-free (a) aluminum and (b) composite cantilever beams from the impact hammer tests using a stationary mounted clamp (clamp 1) and the rotating test stand clamp

Table 1: Test Matrix for Rotating Test Stand Clamp Validation

Case	Beam Type	Boundary Conditions	Test Method	Clamp
1	Aluminum	Free-Free	Modal Hammer - Impact	N/A
2			Modal Hammer - Impact	Rotating Stand
3		Clamped-Free	Clamp 1	
4			Clamp 1	
5			Clamp 2	
6	Composite, 0 wt. % CNT's	Free-Free	Modal Hammer - Impact	N/A
7			Modal Hammer - Impact	Rotating Stand
8		Clamped-Free	Clamp 1	
9			Clamp 1	
10			Clamp 2	

are shown in Figure 4. Although these tests were performed on both the aluminum beam and the composite beam with no CNT's, the trends in each case were similar and therefore only the results for the composite beam are presented in Figure 4 for brevity. The frequency response of the beam in each case was measured and computed using Siglab™, and the test methodology is described as follows: First, the damping was measured using an impact hammer test on a free-free beam to isolate any clamping effects before moving to a clamped-free configuration. Next, the beams were tested as cantilevers by mounting one end in clamp 1 and excited via an impact hammer test, where this same experiment was then repeated using the beam mounted in the rotating test stand clamp. Finally, clamp 1 was mounted to a shaker and the different beams were tested by means of base excitation and compared to the same test using an additional stationary clamp (denoted as clamp 2). From the results in Figure 4, it is evident that the damping in all cases is measured to be approximately 1.25% and there is no statistically significant difference between the results of the free-free tests or any of the clamped-free tests for the composite beam. The standard deviation of the measured damping values for the base excitation results are very small and the standard deviation is relatively larger for the damping measured using the impact hammer tests but still within acceptable limits for the high variation normally found between damping measurements. From the results in Figs. 3 and 4 it is evident that the clamp used on the rotating test stand produces similar results to the other test clamps and methods, and therefore it is reasonable to assume that the rotating test stand and clamp do not significantly affecting the modal parameters measured from the beams reported throughout the remainder of this study.

**Figure 4:** Comparison of the damping measured in the first mode of the composite beam using various testing conditions

Operational Modal Analysis

This subsection presents the results of the modal analysis performed on the rotating beams to calculate the natural frequencies and damping values of the different materials as a function of angular speed from 0 to 500 RPM. Using several cantilever beams with dimensions of $266 \times 12.7 \times 0.2 \text{ mm}$ for each case, three different materials were examined: an aluminum beam serving as the baseline material and two different composite beams reinforced with carbon fiber fabric at a fiber volume fraction of 0.46, the first without CNT's and the second with two weight percent SWCNT's incorporated into the matrix material.

The first three transverse natural frequencies of the different beams as a function of angular speed was first investigated, where the results are presented in Figure 5. The aluminum is shown by a dashed-dot line, the dashed line represents the composite with no CNT's, and the composite infused with two weight percent SWCNT's is denoted using a solid line. To better demonstrate the trends in the natural frequencies of each mode, Fig. 5a shows the results from the third mode, the second mode is illustrated in Fig. 5b, and Fig. 5c presents the results from the first mode. In all three subfigures, it is evident that the natural frequency of each material increases as the angular speed is increased, evidence of the 'spin-stiffening' effect on the beams as a result of centripetal forces acting on the beam at increased rotational speeds [23]. This effect is most noticeable in the first mode shown in Fig. 5c, where the natural frequency in each mode increases by more than one Hertz

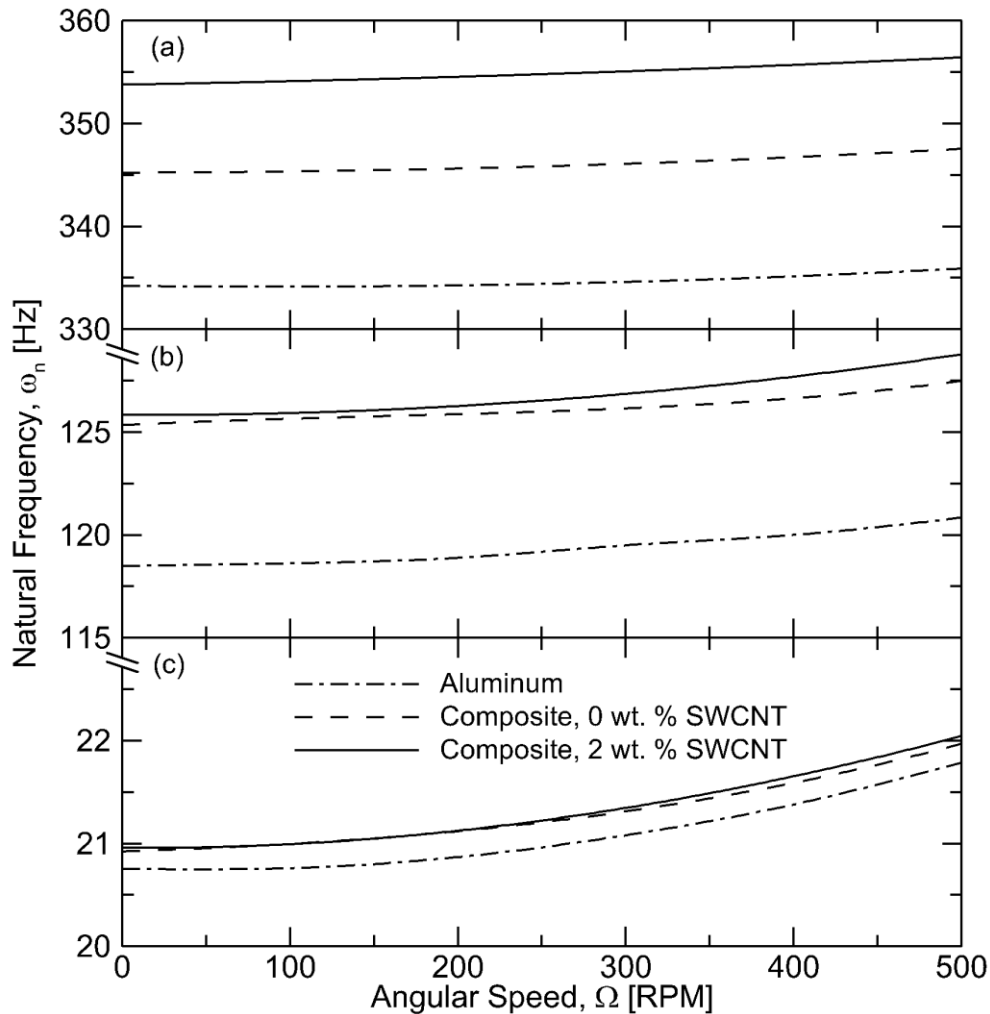


Figure 5: The first three transverse natural frequencies of the aluminum, composite with zero weight percent SWCNT's, and the composite with two weight percent SWCNT's as a function of angular speed. The natural frequencies of the third mode are presented in (a), the second mode in (b), and the first in (c).

when the angular speed increases from 0 to 500 RPM. In the subsequent modes shown in Figs. 5b and 5a this trend is less noticeable because of the scale of the graphs, however in the second and third modes of vibration there is an increase in the natural frequency of about 2.5 and 5 Hertz, respectively, when the angular speed reaches 500 RPM. It is also apparent that the natural frequency of the composite beams are much larger than the aluminum beam, and the composite beam infused with SWCNT's has a higher natural frequency than the composite without CNT's. As carbon-fiber composites are generally stiffer than a similarly shaped aluminum beam, this increase in natural frequency is expected. Additionally, an increase in the natural frequency of the SWCNT-infused composite suggests that the addition of CNT's further enhances the stiffness of the composite beam, a result also observed in previous studies [3,6]. In general, the results in Fig. 5 demonstrate that the beams first three transverse natural frequencies increase with increasing angular speed and that the beams become stiffer when moving from aluminum to composite with no CNT's and from the plain composite to the SWCNT-infused composite material.

Figure 6 presents the measured damping in the first mode of all three material cases as a function of the beam's angular speed from 0 to 500 RPM. As in Fig. 5, the dashed-dot line represents the aluminum beam, the composite with no CNT's is denoted by a short-dashed line, and the solid line is used to show the composite infused with two weight percent SWCNT's. The raw data points at each incremental angular speed in each case are also shown by the various symbols denoted in the legend of Fig. 6, and colors are assigned to each material case to better visualize the data trends. Linear fit lines are used to describe the overall damping trends in each case to better illustrate the damping as a function of angular speed for each material. In the case of the aluminum beam trends shown in Fig. 6, the damping remains relatively constant as a function of angular speed and averages approximately 0.35%. The composite beam with no CNT's has a measured damping value of about 1.25% at 0 RPM, but tends to decrease as the angular speed is increased, reducing to almost 0.6% at 500 RPM. The damping in the composite beam with two weight percent SWCNT's also decreases with increasing RPM, but the damping values are much higher than the case without CNT's. At 0 RPM, the damping in the CNT-infused composite is measured to be about 2.4%,

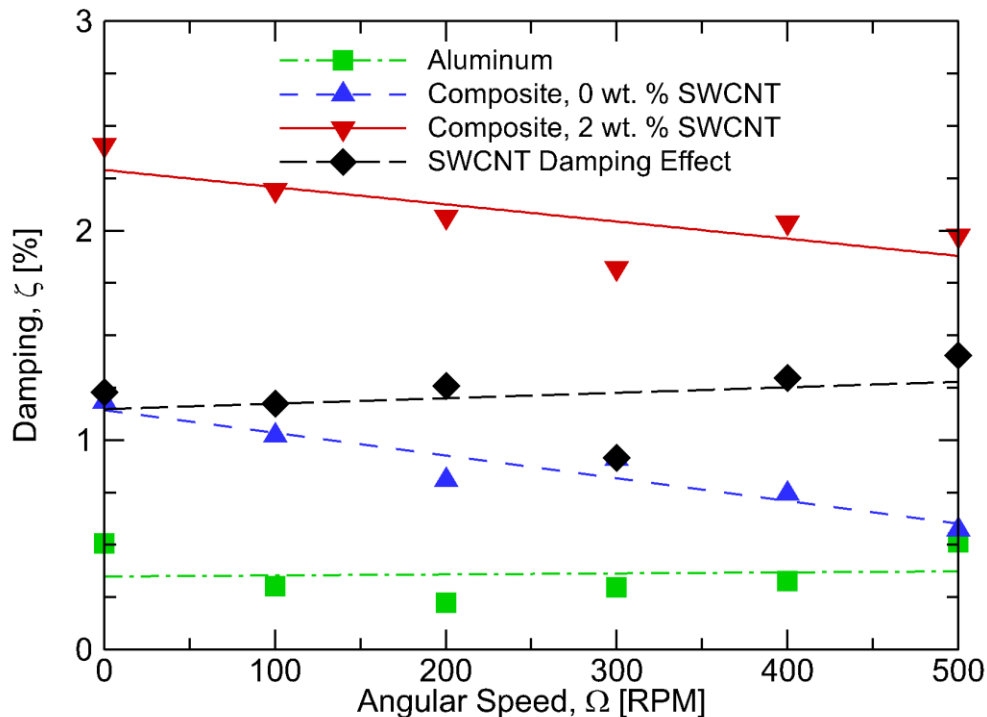


Figure 6: The measured damping in the first transverse mode of the aluminum, composite with zero weight percent SWCNT's, and the composite with two weight percent SWCNT's as a function of angular speed. The difference in the two composite cases with and without CNT's is presented as the 'SWCNT Damping Effect' to visualize the damping increase measured in the fiber-reinforced composite from the SWCNT addition.

and decreases to only 1.9% at 500 RPM. From these values, it is evident that the addition of the CNT's to the composite matrix increases the damping in the composite by an average of 150% throughout the range of tested angular velocities.

In addition, a significant trend is seen when looking at the difference between the measured damping values in the composite beam with and without CNT's versus angular speed, presented in Fig. 6 as the long-dashed black fit line with diamond symbols representing the raw data points. This data set is referred to as the 'SWCNT damping effect' since it is representative of the change in damping between the original fiber-reinforced composite material and the identical fiber-reinforced composite material with the addition of CNT's. The damping difference in the composite as a result of the matrix-embedded CNT's increases with increasing angular speed, suggesting that the SWCNT's have an increasing effect on the material damping as the beam is more rapidly rotated. As was mentioned in the introduction section above, several previous studies investigating CNT damping in composites have found that the damping in the CNT-infused composite increases with increasing material strain. This phenomena might explain the trend in Fig. 6 which shows an increase in the damping measured in the SWCNT-infused composite at higher angular velocities, as the large rotational loads subject the material to increasing strain as the angular speed is increased. Since the material is under strain from these rotational loads, the additional strain needed to initiate the stick-slip action at the CNT-matrix interface is more attainable from the vibration of the beam and might account for the increased damping measured in the beam at the higher angular speeds. Overall, the trends in Figure 6 imply that the addition of CNT's to the matrix of fiber-reinforced composites enhance the damping in the material in a stationary frame and during rotation, with the CNT damping effects increasing as a function of angular speed. Note that the data presented in Figure 6 is based on preliminary test cases and additional tests will be conducted to further increase the robustness of the inferred trends.

CONCLUSIONS

An experimental study was conducted to investigate the effect of Single-Walled Carbon Nanotubes (SWCNT's) on the modal properties of carbon fiber reinforced composite materials during rotation. Operational modal analysis techniques and the eigensystem realization algorithm were applied to analyze vibration measurements recorded from rotating beams excited using an in-house developed experimental test setup utilizing Labview to control and monitor the beams rotation. The results explored the effects of CNT's on the natural frequencies and damping values of aluminum and composite beams as a function of angular speed, and demonstrated that SWCNT's have a beneficial effect on the damping characteristics of rotating composite structures and can further enhance damping at increasingly high angular velocities. This research may be applied to the design of materials used in rotating composite structures such as helicopters blades or wind turbine rotors, where the addition of CNT's to the composite matrix can serve as a means of passive damping augmentation to increase the vibration suppression characteristics of the resulting composite structure.

ACKNOWLEDGEMENTS

This research in this paper is funded in part by the National Science Foundation with Grant No. CBET-0934008, and the U.S. Department of Education through a GAANN fellowship to Caleb DeValve through Award No. P200A060289. Their support is gratefully acknowledged.

REFERENCES

- [1] D. Qian, G. J. Wagner, W. Liu, M. Yu, and R. Ruoff, "Mechanics of carbon nanotubes," *Applied Mechanics Reviews*, vol. 55, no. 6, pp. 495–533, 2002.
- [2] E. T. Thostenson, Z. Ren, and T.-W. Chou, "Advances in the science and technology of carbon nanotubes and their composites: a review," *Composites Science and Technology*, vol. 61, no. 13, pp. 1899–1912, Oct. 2001.
- [3] F. H. Gojny, M. H. G. Wichmann, U. Köpke, B. Fiedler, and K. Schulte, "Carbon nanotube-reinforced epoxy-composites: enhanced stiffness and fracture toughness at low nanotube content," *Composites Science and Technology*, vol. 64, no. 15, pp. 2363–2371, Nov. 2004.
- [4] V. Kostopoulos, A. Baltopoulos, P. Karapappas, A. Vavouliotis, and A. Paipetis, "Impact and after-impact properties of carbon fibre reinforced composites enhanced with multi-wall carbon nanotubes," *Composites Science and Technology*, vol. 70, no. 4, pp. 553–563, Apr. 2010.

- [5] S. Bal and S. S. Samal, "Carbon nanotube reinforced polymer composites—A state of the art," *Bulletin of Materials Science*, vol. 30, no. 4, pp. 379–386, Oct. 2007.
- [6] R. J. Johnson, J. Tang, and R. Pitchumani, "Characterization of damping in carbon-nanotube filled fiberglass reinforced thermosetting-matrix composites," *Journal of Materials Science*, vol. 46, no. 13, pp. 4545–4554, Feb. 2011.
- [7] S. U. Khan, C. Y. Li, N. A. Siddiqui, and J.-K. Kim, "Vibration damping characteristics of carbon fiber-reinforced composites containing multi-walled carbon nanotubes," *Composites Science and Technology*, vol. 71, pp. 1486–1494, 2011.
- [8] M. V. Kireitseu, G. R. Tomlinson, A. V. Ivanenko, and L. V. Bochkareva, "Dynamics and vibration damping behavior of advanced meso/nanoparticle-reinforced composites," *Mechanics of Advanced Materials and Structures*, vol. 14, pp. 603–617, 2007.
- [9] N. A. Koratkar, J. Suhr, A. Joshi, R. S. Kane, L. S. Schadler, P. M. Ajayan, and S. Bartolucci, "Characterizing energy dissipation in single-walled carbon nanotube polycarbonate composites," *Applied Physics Letters*, vol. 87, pp. 1–3, 2005.
- [10] J. Che, W. Yuan, G. Jiang, J. Dai, S. Y. Lim, and M. B. Chan-Park, "Epoxy Composite Fibers Reinforced with Aligned Single-Walled Carbon Nanotubes Functionalized with Generation 0–2 Dendritic Poly(amidoamine)," *Chemistry of Materials*, vol. 21, no. 8, pp. 1471–1479, Apr. 2009.
- [11] L. Liu, A. H. Barber, S. Nuriel, and H. D. Wagner, "Mechanical Properties of Functionalized Single-Walled Carbon-Nanotube/Poly(vinyl alcohol) Nanocomposites," *Advanced Functional Materials*, vol. 15, no. 6, pp. 975–980, Jun. 2005.
- [12] X. Zhou, E. Shin, K. W. Wang, and C. E. Bakis, "Interfacial damping characteristics of carbon nanotube-based composites," *Composites Science and Technology*, vol. 64, pp. 2425–2437, 2004.
- [13] R. M. Lin and C. Lu, "Modeling of interfacial friction damping of carbon nanotube-based nanocomposites," *Mechanical Systems and Signal Processing*, vol. 24, pp. 2996–3012, 2010.
- [14] J.-S. Jang, J. Varischetti, and J. Suhr, "Strain dependent energy dissipation in multi-scale carbon fiber composites containing carbon nanofibers," *Carbon*, vol. 50, no. 11, pp. 4283–4277, May 2012.
- [15] E. Reynders, "System Identification Methods for (Operational) Modal Analysis: Review and Comparison," *Archives of Computational Methods in Engineering*, vol. 19, no. 1, pp. 51–124, Feb. 2012.
- [16] P. Mohanty and D. J. Rixen, "Operational modal analysis in the presence of harmonic excitation," *Journal of Sound and Vibration*, vol. 270, no. 1–2, pp. 93–109, Feb. 2004.
- [17] P. Mohanty and D. J. Rixen, "Modified ERA method for operational modal analysis in the presence of harmonic excitations," *Mechanical Systems and Signal Processing*, vol. 20, pp. 114–130, 2006.
- [18] L. Hermans and H. Van der Auweraer, "Modal testing and analysis of structures under operational conditions: industrial applications," *Mechanical Systems and Signal Processing*, vol. 13, no. 2, pp. 193–216, 1999.
- [19] G. H. James, T. G. Carne, and J. P. Lauffer, "The Natural Excitation Technique (NExT) for modal parameter extraction from operating structures," *The International Journal of Analytical and Experimental Modal Analysis*, vol. 10, no. 4, pp. 260–277, 1995.
- [20] N. Granick and J. E. Stern, "Material damping of aluminum by a resonant-dwell technique," Greenbelt, Maryland, 1965.
- [21] R. F. Gibson and R. Plunkett, "A forced-vibration technique for measurement of material damping," *Experimental Mechanics*, vol. 17, no. 8, pp. 297–302, 1977.
- [22] J. M. Lee and K. G. McConnell, "Experimental cross-verification of damping in three metals," *Experimental Mechanics*, vol. 15, no. 9, pp. 347–353, 1975.
- [23] A. D. Wright, C. E. Smith, R. W. Thresher, and J. L. C. Wang, "Vibration modes of centrifugally stiffened beams," *Journal of Applied Mechanics*, vol. 49, no. 1, pp. 197–202, 1982.